JOURNAL OF APPLIED ELECTROCHEMISTRY 2 (1972) 265–273

The mechanism of discharge of sintered plate cadmium electrodes

R. D. ARMSTRONG,* A. D. SPERRIN,† F. L. TYE† and G. D. WEST*

* *Electrochemistry Research Laboratories, Department of Physical Chemistry, University of Newcastle upon Tyne, Newcastle upon Tyne, U.K.*
† *Central Laboratories, Ever Ready Co. (G.B.) Ltd., London, U.K.*

Received 13 March 1972

Sintered plate Cd electrodes have been studied in alkaline solutions using potentiostatic and galvanostatic techniques. The behaviour is, in many ways, similar to that of a flat Cd electrode. A pseudo steady-state current is found due to the dissolution of Cd as $Cd(OH)_4^{2-}$. At more anodic potentials passivation occurs due to the solid state formation of $Cd(OH)_2$. This model can account for the results obtained on galvanostatic discharge.

1. Introduction

The mechanism of the cadmium electrode in alkaline solution is of considerable interest in relation to the operation of the commercial Ni–Cd battery. In spite of previous studies there are still uncertainties concerning some aspects of this mechanism.

From work on flat Cd electrodes it has been shown [1, 2, 3, 4] that the discharge reaction involves a solution soluble complex which is probably $Cd(OH)_4^{2-}$ [5, 8], though $Cd(OH)_3^-$ has also been suggested [6, 7, 9].

The mechanism of passivation of the Cd electrode has also been discussed [1, 2, 3, 10, 11]. Thus a number of authors [3, 10] have taken the view that this passive layer is formed via a dissolution–precipitation mechanism. However it should be noted that Devanathan and Lakshmanan [10] used an $i\,\tau^{\frac{1}{2}}$ relationship which is in error [12]. From work on Cd amalgams [11] and from rotating disc studies on Cd [1], evidence was found for a solid state mechanism of film formation.

Most mechanistic studies have been performed using either flat Cd electrodes or amalgams; their value, in the context of the real battery system, is thus reduced. The working of the real, sintered plated electrode, is less well understood.

Theoretical studies on the electrochemical behaviour of porous electrodes [13, 14, 15, 16] are not directly applicable to this case as solid $Cd(OH)_2$ accumulates inside the body of the electrode throughout the discharge [17]. The effect of this precipitate on the discharge behaviour is uncertain.

Harivel *et al* [18], in an extensive study of the behaviour of the sintered negative electrode, have discussed the efficiency of the electrode with reference to charge rate, electrolyte concentration and temperature. They suggest that the inefficiency on discharge is due to a limiting of the ionic diffusion by precipitated $Cd(OH)_2$. They further show that crystals of non-oxidized Cd metal exist within the sinter, the size of these crystals increasing with the number of charge/discharge cycles. Using an X-ray technique they estimated a surface area of 8·3 $m^2\ g^{-1}$ of active material for a fully loaded sinter. This area may be compared with 7·8 $m^2\ g^{-1}$ of active material measured by a B.E.T. adsorption method. A B.E.T. adsorption technique for measurement of surface areas has been described by Salkind *et al* [19], who find areas ranging from 1 to 13 $m^2\ g^{-1}$ of active material, for uncycled, dis-

charged electrodes. The large variation in area decreased with cycling and was attributed to a redistribution of active material through the sinter. This redistribution has also been shown using X-ray and light microscopy.

Bro and Kang [20] have measured discharge profiles in porous Cd electrodes using an analytical technique. They find that the extent of reaction within the sinter is strongly influenced by the current density of discharge. They suggest that the discharge efficiency was limited due to choking of the sinter by precipitated $Cd(OH)_2$.

Casey and Vergette [21] interpret the performance of negative sinters in terms of a physical model and find that the efficiency of the sinter may be understood in terms of free pore volume accessible to the electrolyte. They further suggest that the amount of available active material falls off rapidly with increased loading of the sinter.

The present investigation was undertaken in an attempt to clarify the mechanism of discharge of the sintered negative electrode, with special reference to the role of the solid $Cd(OH)_2$ known to be formed within the matrix of the sinter during the course of a discharge.

2. Experimental

The porous electrodes consisted of nickel powder sintered on to a metal support, of approximate external dimensions 1 cm × 1 cm × 0·65 mm, impregnated after the method of Fleischer [22] and Horn [23]. Care was taken during the impregnation to minimize corrosion of the sintered matrix, with subsequent formation of $Ni(OH)_2$. The amount of residual $(NO_3)^-$ in the plates was reduced by careful washing. Analysis showed in all cases the amount of $Ni(OH)_2$ in the plates to be less than 0·5 mg cm^{-2} and the amount of unconverted $(NO_3)^-$ to be less than 0·01 mg cm^{-2}.

The flat plate electrodes were prepared from Cd sheet, purity 6 N (Koch–Light); these electrodes were mechanically polished with γ-alumina (particle size 1–5 μm) before use.

All measurements were made in a glass cell using Hg/HgO reference electrodes in the same solution and two nickel counter electrodes.

The solutions were 3% and 30% wt/wt in potassium hydroxide, made up using L.R.B. Pearce technical grade flake and singly distilled water. Table 1 shows a typical analysis of the potassium hydroxide used.

All solutions were deoxygenated with nitrogen before use.

Table 1. *Analysis of L.R.B. Pearce technical grade flake*

KOH	88–90%
K_2CO_3	0·3%
KCl	0·04%
Cl	0·02%
K_2SO_4	No precipitate with $BaCl_2$
SiO_2	0·005%
Fe_2O_3	0·001%
NiO	0·002%
H_2O	Balance

Measurements were made at the ambient temperature of the laboratory (21 ± 2°C).

Potentiostatic current voltage curves were measured using a Chemical Electronics pottentiostat (Type TR40/3A). Constant potential discharges were obtained using the potentiostat

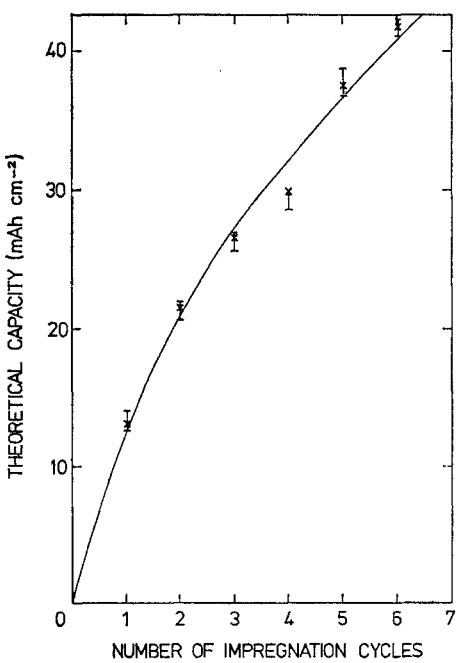

Fig. 1. Change in theoretical capacity of sinters with number of impregnation cycles. X, values from analysis; I, range of 8 weight gain results.

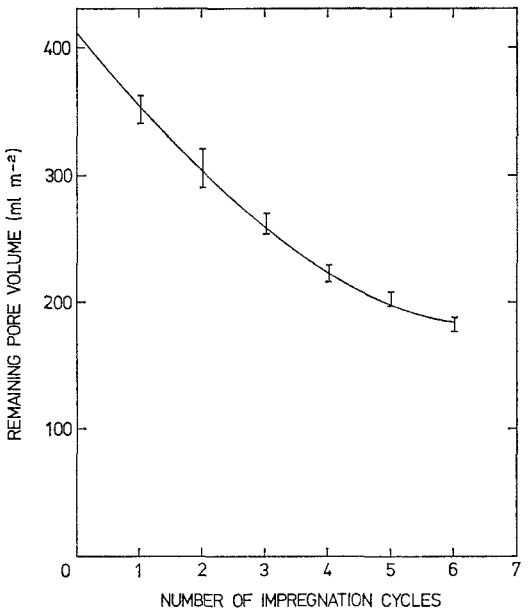

Fig. 2. Change in remaining pore volume of sinters with number of impregnation cycles. I, range of 8 determinations.

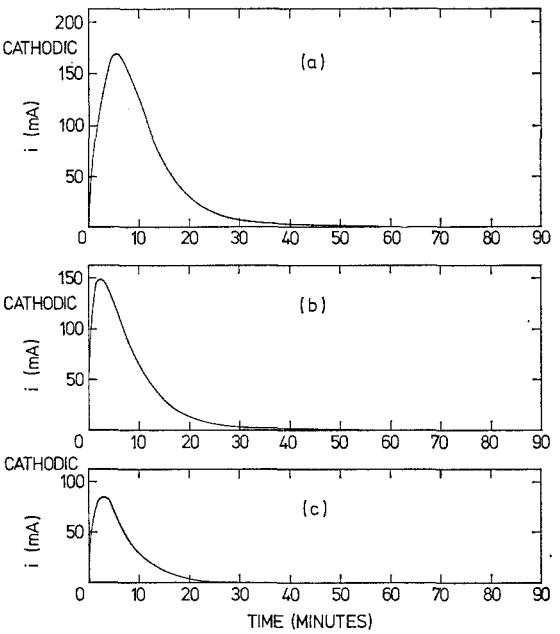

Fig. 3. Typical potentiostatic charge curves for sintered electrodes in 30% KOH, at −1000 mV (vs. Hg/HgO). Efficiencies:
(a) 100·5%, 6 cycles of impregnation.
(b) 97%, 3 cycles of impregnation.
(c) 96%, 2 cycles of impregnation.

in conjunction with a Y-t recorder (Servoscribe). Before each run the electrodes were polarized at −1000 mV (w.r.t. Hg/HgO) until the current had reached a steady value.

Galvanostatic charge/discharge curves at various currents were obtained using a conventional transistorized constant current unit in conjunction with the Y-t recorder.

In all cases the measurements were performed using uncycled electrodes only.

3. Results and discussion

3.1. *Characterization of the sinters*

The theoretical capacity of the sinters estimated separately by analysis and weight gain were in excellent agreement. Fig. 1 shows the change in theoretical capacity of the sinters and Fig. 2. the change in remaining pore volume (measured by water uptake), with the number of impregnation cycles.

3.2. *Potentiostatic measurements*

Sintered electrodes were charged at −1000 mV (vs. Hg/HgO); Fig. 3 shows typical charge curves. The rising portion is probably due to an increase of the active area due to the nucleation and growth of Cd crystals, the falling portion corresponding to a depletion of reducible material and overlap of the crystals. The charging process was found to be very nearly 100% efficient and thus it would appear that hydrogen evolution is not an important reaction at this potential.

Electrodes charged potentiostatically were discharged at various constant potentials. Fig. 4 shows the typical behaviour in which, at potentials just anodic to the $Cd/Cd(OH)_2$ potential, a fairly constant initial current is maintained followed by a steady falling off to near zero. The charge under the curves, at times up to 30 minutes, represents only about 75% of the theoretical capacity. This inefficiency must be attributed to choking of the pores or blocking of the active surface by $Cd(OH)_2$. The currents maintained are in agreement with those observed after 1 minute during the measurements described below.

Potentiostatic *I–E* curves were measured on

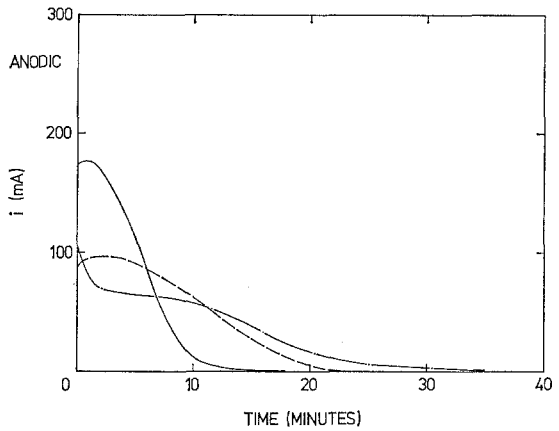

Fig. 4. Typical constant potential discharges on sintered electrodes (3 impregnation cycles) in 30% KOH. Average of 3 separate experiments.

– · – · – · – at −880 mV
– – – – – at −870 mV } vs. Hg/HgO
——— at −860 mV

fully charged sintered and flat plate electrodes, each potential being maintained for 1 minute. Figs. 5 and 6 show typical behaviour. These curves are similar to those already reported for rotating disc electrodes [1], where the currents

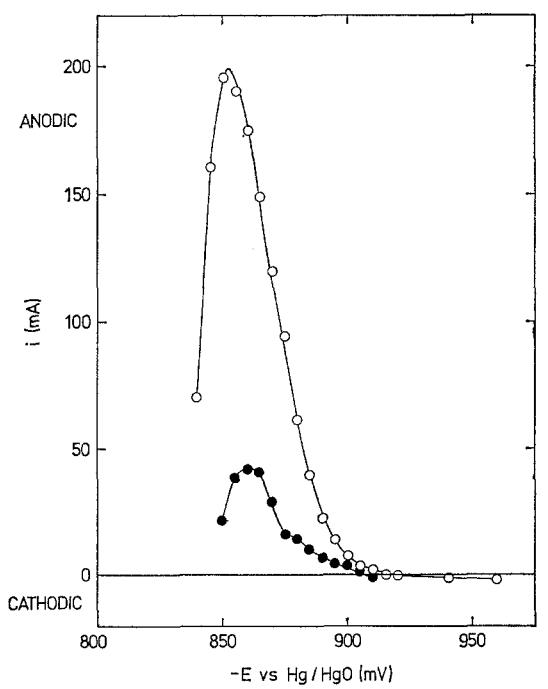

Fig. 5. Typical *I–E* curves for sintered electrodes in 30% KOH. Average of 3 experiments.
○, 6 impregnation cycles
●, 1 impregnation cycle

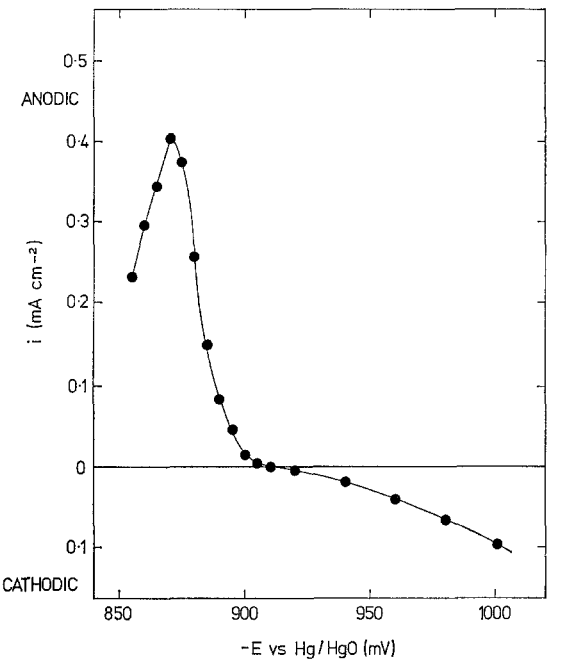

Fig. 6. Typical *I–E* curve for flat plate electrode in 30% KOH. Average of 3 experiments.

were shown to be due to the dissolution of Cd as $Cd(OH)_4^{2-}$ and the same explanation must hold here. Comparison of the curves shows that the potential distribution effects within the sinter are small, since the peak voltages for the sintered electrodes are shifted by less than 10 mV compared with the flat plate. Calculation shows that the maximum potential difference throughout the sinter is less than 15 mV. The fall in current thus cannot be due to diffusion limitations within the pores, neither can it be predominantly due to consumption of cadmium, although this is a factor, as up to 45% of the total is consumed in making the measurements (compare Fig. 8).

Fig. 7 shows the change in measured peak current with level of impregnation; the general trend is similar to that of Fig. 1, except that the curvature is greater. This is probably due to the real surface area tending toward a maximum at higher levels of impregnation due to excessive loading.

An estimate of the true area of the sinters was made by direct comparison of the peak heights shown in Figs. 5 and 6. A value of about 1 $m^2\ g^{-1}$ of active material $Cd(OH)_2$ is obtained, allowing for a roughness factor of 2 for the flat

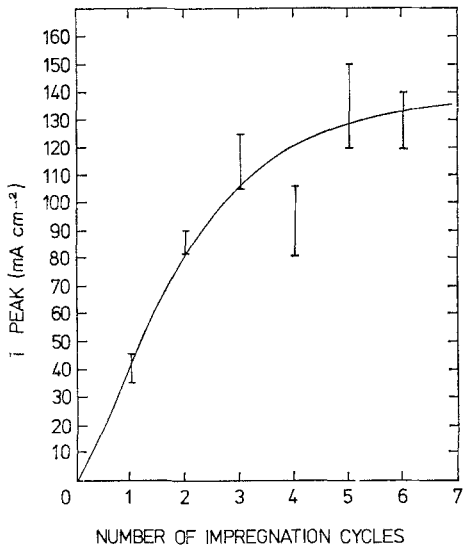

Fig. 7. Change in measured peak current with number of impregnation cycles for sintered electrodes in 30% KOH. I, range of 3 determinations.

plate. This comparison allows for no difference in diffusion layer thickness between the flat plate (with $\delta \simeq 10^{-2}$ cm for natural convection) and the sinter, which would have δ probably less than or equal to the average pore diameter of the matrix, in this case about 10^{-3} cm [24].

Potentiostatic *I–E* curves were obtained as

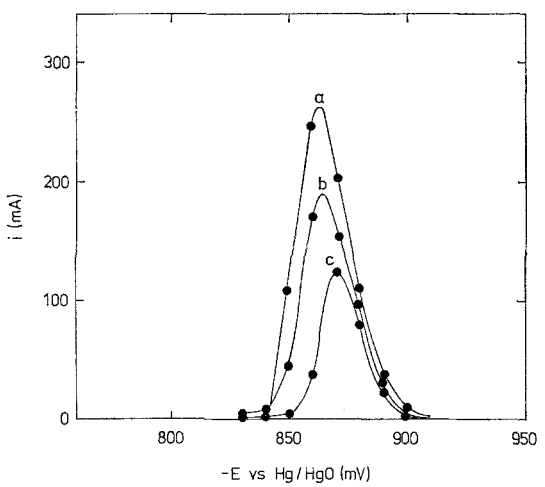

Fig. 8. Typical behaviour of sintered electrodes (impregnation cyles) after various degrees of galvanostatic discharge in 30% KOH. Average of 3 separate experiments.
A, no discharge.
B, 20% discharge.
C, 40% discharge.

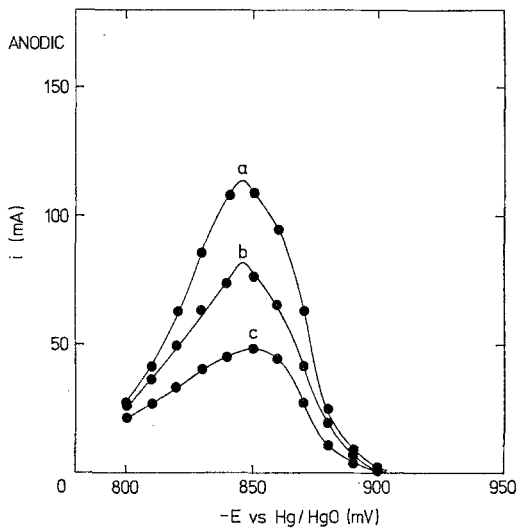

Fig. 9. As Fig. 8 but for 3% solutions.

described previously, for sinters after varying amounts of galvanostatic discharge. Figs. 8 and 9 show the behaviour for 30% and 3% solutions. The currents in the 3% solution are only about one-third of those in the 30%; for a reversible dissolution reaction with the formation of hydroxy complexes a dependence of this sort on $[OH^-]$ would be expected. The peaks for the 3% solution are broader, showing a greater potential distribution within the sinter for the more dilute solution.

The steady fall in peak heights must be taken as demonstrating a decrease in active area due to electrochemical dissolution of the active material. There may also be a certain amount of blockage of the surface due to precipitated $Cd(OH)_2$.

3.3. *Galvanostatic discharge*

Galvanostatic charge and discharge curves were measured for sintered and flat electrodes. Typical charge and discharge curves are shown in Figs. 10 and 11. The voltage overshoot in the charge curves is reproducible but becomes progressively smaller as the charge current is reduced; it is probably associated with nucleation of hydrogen bubbles.

Charge efficiencies (w.r.t. the theoretical capacity) for sintered electrodes were measured and found to be strongly dependent on charge

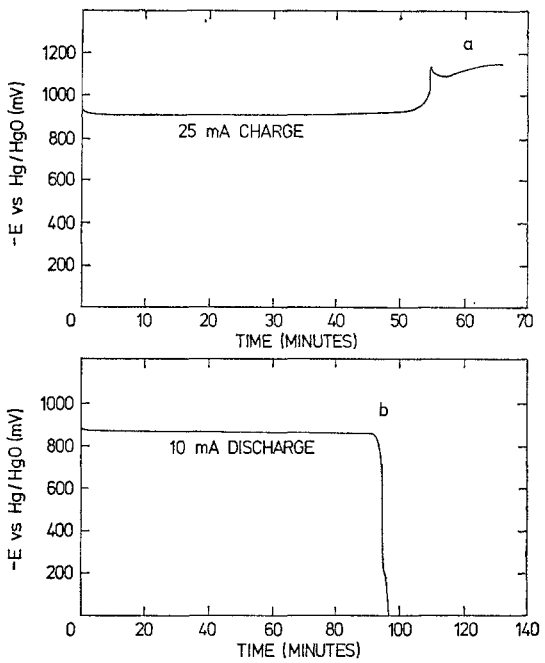

Fig. 10. Typical (a) charge, and (b) discharge curves for sintered (4 impregnation cycles) electrodes in 30% KOH.

current and extent of impregnation; Fig. 12 demonstrates this effect.

The efficiences for impregnations 4 and 6 were, within the limits of accuracy of the experiment,

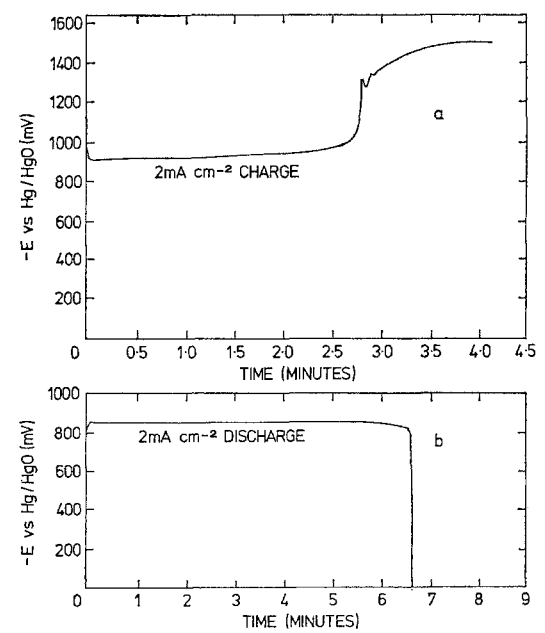

Fig. 11. As Fig. 10 but for flat plate electrodes in 30% KOH.

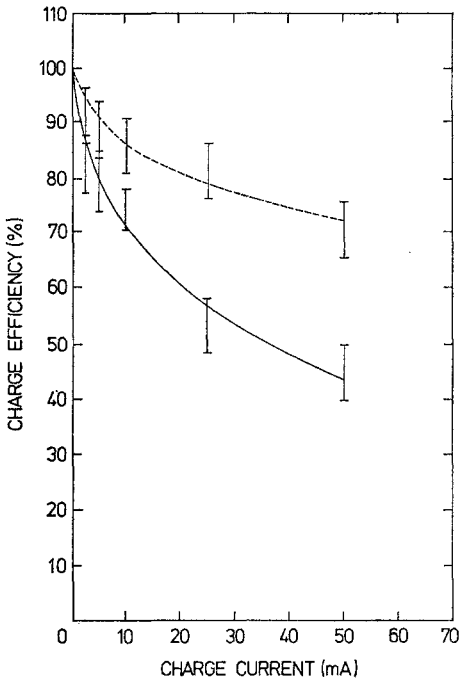

Fig. 12. Change in charge efficiency with charge current, for sintered electrodes in 30% KOH,
——— 1 impregnation cycle;
– – – – – 4 and 6 impregnation cycles. I, range of 12 determinations.

the same. The charge accepted was estimated using a time τ, equal to the time required to reach a voltage half way between the two steady values; care was taken not to overcharge the electrode for any length of time.

Fig. 13 shows the effect of lowering the charge current on a sintered electrode: it is obvious that even after the inflection in the charge curve, corresponding to the onset of hydrogen evolution, the electrode will accept a further quantity of charge. Thus it may be seen that the apparent inefficiency of the sintered electrodes on charge is due to a premature onset of hydrogen evolution, the extent of this inefficiency being strongly dependent on the charge current density.

Discharge efficiencies of sintered electrodes, measured to a -800 mV (vs. Hg/HgO) endpoint were found to be dependent on both the current used for the initial charge and the discharge. Fig. 14 shows typical behaviour. A dependence of this sort has been reported previously [18].

Electrodes were discharged at constant

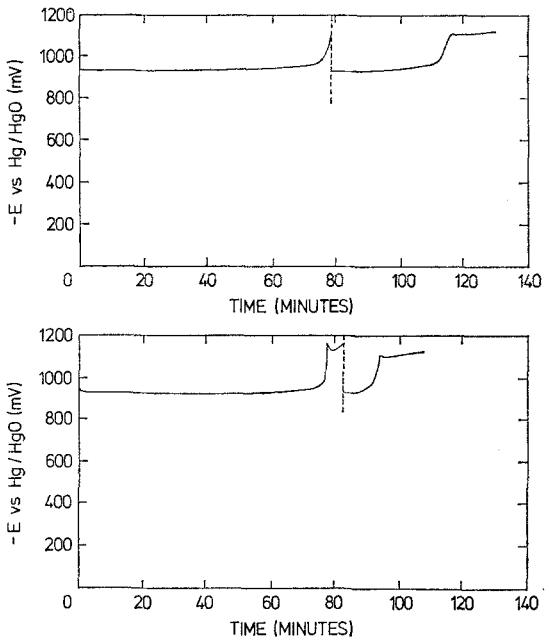

Fig. 13. Effect of lowering charge current on the charge behaviour of a sintered electrode (4 impregnation cycles) in 30% KOH, – – – – corresponds to a reduction of charge current from 25 mA to 5 mA.

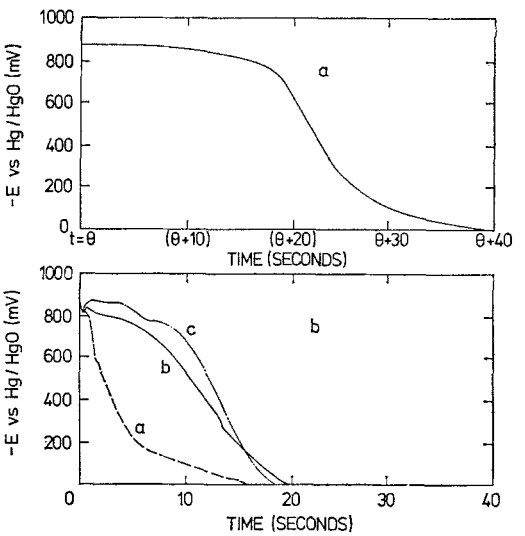

Fig. 15. (a) Final portion of typical discharge curve for sinter in 30% KOH.
(b) Typical behaviour of sintered electrodes in 30% KOH after open circuit recovery. Both curves are for 25 mA discharge of sinter which had 4 cycles of impregnation.
(A) electrode discharged to −600 mV; open circuited until potential reaches a steady value, then fully discharged; – – – – (B) as in (A) but discharged to −800 mV ——— (C) as in (B) but open circuit stand greater than 15 hours. – · – · – · –

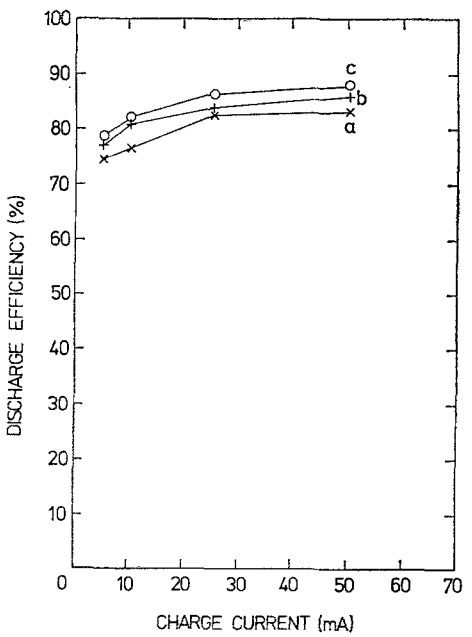

Fig. 14. Typical dependence of discharge efficiency on charge and discharge current for sintered electrodes (4 impregnation cycles) in 30% KOH. A = 25 mA; B = 10 mA; C = 5 mA discharge rates.

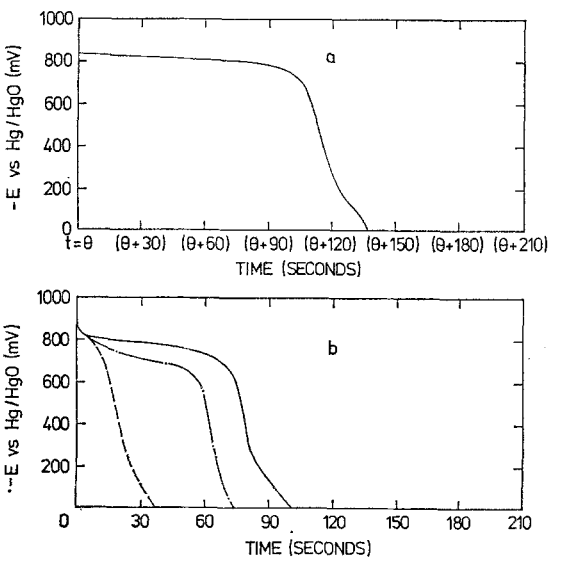

Fig. 16. As Fig. 15 but in 3% KOH.

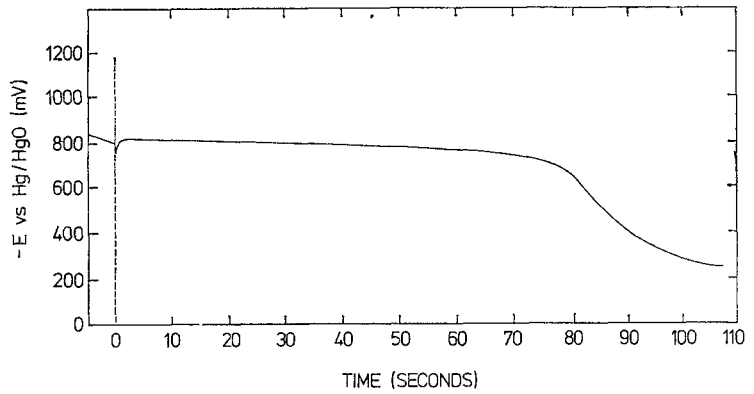

Fig. 17 Effect of lowering discharge current on the discharge behaviour of a sintered electrode (4 impregnation cycles) in 30% KOH; – – – – corresponds to a lowering of the current from 25 mA to 5 mA.

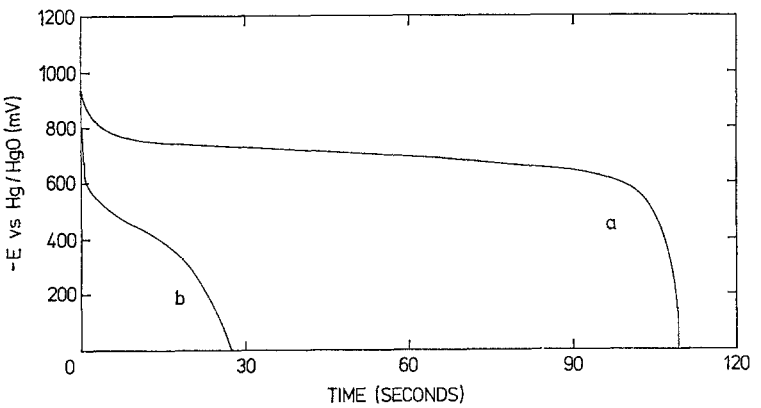

Fig. 18. Typical curves for high rate discharge (500 mA) on sintered electrodes (4 impregnation cycles) in (a) 30% KOH; (b) 3% KOH.

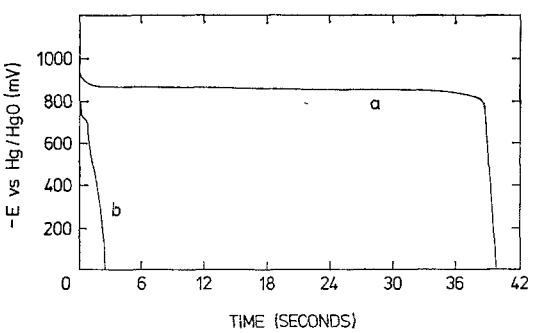

Fig. 19. Typical curves for high rate discharge (5 mA flat on plate cm^{-2}) electrodes in: (a) 30% KOH; (b) 3% KOH.

current until they had reached a particular potential w.r.t. the Hg/HgO reference electrode. They were then switched to open circuit and the electrode potential was allowed to recover to a steady value. The recovery in all cases was rapid but some electrodes were left for 15 minutes, and others 15 hours, prior to attempting further discharge. The results of the attempted discharges are shown in Fig. 15(b) and 16(b) for 30% and 3% KOH respectively.

It is obvious that the extra capacity delivered on the second discharge is extremely small and, in fact, it represented typically less than 0·5% of the total capacity of the electrode although as much as 20% of the total theoretical capacity remained undischarged.

The shape and area under the curves in Figs. 15(b) and 16(b) are little different from the −800 mV to 0 mV and −600 mV to O mV portions of the normal discharge curves shown in Figs. 15(a) and 16(a).

Thus it is seen that once an electrode is discharged to potentials less than 800 mV w.r.t.

Hg/HgO it shows no sign of recovery, even over extended stand times. Therefore diffusion limitations cannot account for the failure to discharge fully the cadmium in a sintered plate electrode.

Fig. 17 shows that, even if the current density is reduced subsequent to the electrode potential reaching 800 mV, the number of coulombs that can be withdrawn from the electrode is not significantly increased. Similar behaviour occurred in 3% KOH solution.

These results confirm the deduction made from the potentiostatic *I–E* data that failure of the cad mium electrode on discharge is due to blocking of the active surface by a layer of $Cd(OH)_2$.

High rate discharge capacities for sintered and flat plate electrodes were measured in 30% and 3% solutions. The discharge capacity was greatly reduced by lowering the electrolyte concentration (Figs. 18 and 19). This sort of dependence on $[OH^-]$ indicates that the mechanism of discharge prior to passivation involves the formation of hydroxy complexes.

A consideration of the process of impregnation [22, 23], along with previous work [4, 18, 21], suggests that a reasonable model for the charged sinter would consist of discrete crystallites of Cd held in the void spaces of the nickel sinter.

A mechanism for the galvanostatic discharge of a sintered electrode is proposed as follows:

(i) Dissolution of the active material as solution soluble hydroxy complexes. These complexes may be reprecipitated within the body of the sinter as solid $Cd(OH)_2$.

(ii) As the dissolution proceeds, the area of the active Cd is reduced, either by direct dissolution of the crystallites or a blocking of the surface by solid (precipitated) $Cd(OH)_2$. The polarization within the sinter increases until a potential is reached at the surface such that a new reaction, that is, direct growth of $Cd(OH)_2$ on to the Cd, is possible. This solid film grows with a rate determined by the current until it reaches a thickness such that insufficient current can be drawn from the reaction and some other process, in this case O_2 evolution, must occur.

It is the formation of this solid, insoluble film on the surface of the active material which we consider to be the true cause of passivation.

Acknowledgement

This work was carried out at the Central Laboratories of The Ever Ready Co. (G.B.) Ltd., and the authors thank P. Kelson for guidance and assistance, and the Directors of the Ever Ready Co. (G.B.) Ltd., for permission to publish the work.

References

[1] R. D. Armstrong and G. D. West, *J. Electroanal. Chem.*, **30** (1971) 385.
[2] R. D. Armstrong, J. D. Milewski, W. P. Race and H. R. Thirsk, *J. Electroanal. Chem.*, **21** (1969) 517.
[3] Y. Okinaka, *J. Electrochem. Soc.*, **117**, (1970) 289.
[4] J. L. Weininger and M. W. Breiter, "Power Sources 1966" (Ed. D. H. Collins), Pergamon Press, p. 269 (1967).
[5] P. E. Lake and J. M. Goodings, *Canad. J. Chem.*, **36** (1958) 1089.
[6] P. C. Milner and U. B. Thomas, in 'Advances in Electrochemistry and Electrochemical Engineering', Vol. 5 (Ed. C. W. Tobias), Interscience, New York, p.1 (1967).
[7] D. Dryssen and P. Lumme, *Acta. Chem. Scand.*, **16** (1962) 1785.
[8] D. E. Ryan, J. R. Dean and R. M. Cassidy, *Canad. J. Chem.*, **43** (1965) 999.
[9] R. E. Visco and R. M. Sonner, *Extended Abstracts*, Battery Division of Electrochemical Society, Fall Meeting, 1969, p. 18.
[10] M. A. V. Devanathan and S. Lakshmanan, *Electrochim. Acta*, **13** (1968) 667.
[11] M. Fleischmann, K. S. Rajagopalan and H. R. Thirsk, *Trans. Faraday. Soc.*, **59** (1963) 741.
[12] R. D. Armstrong, *J. Electroanal. Chem.*, **28** (1970) 221.
[13] J. E. Dunning and D. N. Bennion, *Proceedings of Advances in Battery Technology Symposium* December 5, 1969, Vol. 5, p. 135.
[14] E. A. Grens, *Electrochim. Acta*, **15** (1970) 1047.
[15] J. S. Newman and C. W. Tobias, *J. Electrochem. Soc.*, **109** (1962) 1183.
[16] R. C. Alkire, E. A. Grens and C. W. Tobias, *J. Electrochem. Soc.*, **116** (1969) 1183.
[17] S. U. Falk, *J. Electrochem. Soc.*, **107** (1960) 661.
[18] J. P. Harivel, B. Morignat and J. Migeon, 'Batteries' **2** (Ed. D. H. Collins), Pergamon Press, p. 107 (1965).
[19] A. J. Salkind, H. J. Canning and M. L. Block, *J. Electrochem. Soc.*, **2** (1964) 254.
[20] P. Bro and H. Y. Kang, *J. Electrochem. Soc.*, **118** (1971) 519.
[21] E. J. Casey and J. B. Vergette, *Electrochim. Acta.*, **14** (1969) 897.
[22] A. Fleischer, *J. Electrochem. Soc.*, **94** (1948) 289.
[23] L. Horn, *Chem.-Ing.-Techn.*, **38** (1966) 660.
[24] J. C. Duddy and A. J. Salkind, *J. Electrochem. Soc.*, **108** (1961) 717.